Journal of Applied Polymer Science

In Situ Small Angle X-ray Scattering Study on Structural Evolution of Crosslinked Polytetrafluoroethylene During Deformation

Xiaoyun Li,[1] Feng Tian,[1] Chunming Yang,[1] Zhongfeng Tang,[1] Xiaran Miao,[1] Guozhong Wu,[1] Xiuhong Li,[1] Jie Wang,[1] Liangbin Li[2]

[1]Shanghai Synchrotron Radiation Facility, Shanghai Institute of Applied Physics, Chinese Academy of Sciences, Shanghai, China
[2]National Synchrotron Radiation Laboratory and College of Nuclear Science and Technology, University of Science and Technology of China, Hefei, China
Correspondence to: X. Li (E-mail: lixiuhong@sinap.ac.cn)

ABSTRACT: The structural evolution of virgin and crosslinked polytetrafluoroethylene (PTFE) during stretching was studied by *in situ* synchrotron small-angle X-ray scattering (SAXS). Both yield and tensile stress of crosslinked PTFE increased with increasing crosslinking density. During stretching, for virgin PTFE, amorphous chains gradually turned to tensile direction at early stage, perpendicularly arranged lamellar stacks appeared at high strains (>140%). While for crosslinked PTFE, lamellar structure was observed even at lower strains; with increasing irradiation dose, the lamellar structure became obvious and the long period decreased. Four-point SAXS patterns were observed only in 3000kGy-dosed PTFE during deformation, which indicated that an alternately tilted lamella arrangement called herringbone structure was formed. Radiation dose induces crosslinked networks formed, which can carry part of local stress during deformation, resulting in the increase of yield and tensile stress. Crosslinking density is an important factor on structural evolution. In addition, a deformation mechanism of different crosslinked PTFE is proposed. © 2013 Wiley Periodicals, Inc. J. Appl. Polym. Sci. **2014**, *131*, 39883.

KEYWORDS: morphology; structure-property relations; X-ray

Received 7 June 2013; accepted 21 August 2013
DOI: 10.1002/app.39883

INTRODUCTION

Polytetrafluoroethylene (PTFE) is a complicated semicrystalline polymer, which is widely used in many fields due to chemical stability, low friction coefficients, heat resistance, considerable biocompatibility, and many other properties. But its application is limited under radiation environment due to highly sensitive to radiation for PTFE.[1] Under air or vacuum, very low radiation dose leads to PTFE main chain scission, which reduces dramatically molar mass at room temperature.[2] As a result, PTFE is of brittleness and the mechanical properties are degraded.[3] However, in oxygen-free atmosphere and above the melting points, the chains of PTFE can be crosslinked under radiation.[1,4–6] After crosslinking, the light transmittance enhances in the infrared range.[7] And the coefficients of abrasion, permanent creep, radiation resistance, yield strength, and Young's modulus were improved greatly.[5–7]

It is well known that there is some relationship between structure and properties in semicrystalline polymer materials. The crystalline phase or phase transition may bring some effect to properties. For virgin PTFE, it behaves complex crystalline phase. Four crystalline structures were observed: Phase I, Pseudo-hexagonal crystal; Phase II, triclinic crystal; Phase III, planar zig-zag crystal; and Phase IV, Hexagonal crystal.[8] At 19°C, the first-order transition from phases II to IV was an unraveling in the helical conformation. And at 30°C, PTFE exhibited the phase I structure due to further rotational disordering and untwisting of the helices.[9–11] Crosslinked PTFE also exhibits four phases. Chemical transformations and changes of crosslinked PTFE have been studied by different ways. From WAXS patterns of PTFE irradiated, it was found that there was a tendency of a decreasing crystallinity with increasing dose.[1] This was confirmed by differential scanning calorimetry (DSC). The Fourier transform infrared spectroscopy (FTIR) demonstrated that new C=C bond appeared in crosslinked PTFE, and trifluoromethyl branches whose concentration was much higher after irradiation in molten state.[12] Oshima had studied radiation crosslinked PTFE by ^{60}Co γ-ray using electron spin resonance spectroscopy (ESR). Free radicals was formed and then converted into peroxy radicals by reaction with oxygen at 24°C.[6] In addition, it was proposed that most radicals were trapped and formed in crosslinked amorphous region, and then

© 2013 Wiley Periodicals, Inc.

these region formed network structure to enhance the mechanical property.

Indeed, the structure–mechanical property relationship of PTFE introduced academic interest., and it has been studied by many researchers. Recently, Atsuhiro developed a plastic optical fiber using polytetrafluoroethylene-*co*-(perfluoroethylvinylether) with excellent heat resistance and dimensional stability. A lamella crystal was formed in this polymer fiber by *in situ* SAXS and WAXS methods.[13] Brown studied systematically the fracture and microstructure evolution of PTFE during deformation at different temperature. It showed that failure behavior and microstructure were correlated to temperature-induced phase transitions.[8] Kyung studied structural development of PTFE films in multistage stretching. It was found that the higher stretch ratio is, the higher orientation, regardless of uniaxial or biaxial stretch.[14]

Although a lot of work was performed to investigate the structural evolution of virgin (noncrosslinked) PTFE during deformation, there were few studies about mechanism of deformation on the crosslinked structure, as far as we know. In order to understand the relationship of structure evolution, crosslinking density and mechanical property in crosslinked PTFE, in this research, virgin PTFE and crosslinked PTFE with different radiation dose was investigated by SAXS technique combined with an in-situ uniaxial stretching apparatus.

EXPERIMENTAL

Material and Preparation

The crosslinked PTFE was prepared by electron beam (EB) radiation in the molten state of PTFE at 335 ± 5°C in nitrogen gas atmosphere. The molecular weight of PTFE is 1.6×10^6 g/mol. The dose was changed from 300 to 3000 kGy to prepare samples with various crosslinking densities. For our samples, the light transparencies enhanced increased with irradiation dose either. Sample numbered XPTFE-3000 (that means a dose of 3000 kGy), and XPTFE-3000 has a best transparency. It indicates that crosslinking density increases as EB irradiation dose increasing.[7]

Characterization Methods

A typical tensile profile of virgin and crosslinked PTFE specimens was prepared with a length of 30 mm and neck width of 12 mm. A home-made uniaxial tensile apparatus was used for deformation. The uniaxial stretching guarantees that the focused X-ray beam illuminates the same sample position during stretching. The tensile speed was 1.16 μm/s. All experiments were carried out at room temperature. The transmission-geometry SAXS data were acquired immediately after the preset strain value was reached during the deformation process. *In situ* SAXS tensile experiments were performed at beamline BL16B1 at Shanghai Synchrotron Radiation Facility (SSRF). The incident X-ray wavelength was 0.124 nm. The 2D SAXS patterns were recorded by Mar165 CCD with pixel size of 80×80 μm. A sample-to-detector distance of 5265 mm was calibrated by a beef tendon specimen. All X-ray scattering data were corrected for background scattering, X-ray absorption, and sample thickness. Fit2D software was used to analyze SAXS patterns and thus obtained the one-dimensional integrated intensity curves. In consideration of the stretching direction, the equatorial intensities were integrated over $-15° \leq \psi \leq 15°$ (equatorial direction is along the stretching direction), while the meridional intensities were obtained by integration over $75° \leq \psi \leq 105°$, where ψ denotes the azimuth angle.

RESULTS AND DISCUSSION

Stress-Strain Curves

It is well known that EB radiation would affect the mechanical properties and microstructure evolution of PTFE. Figure 1 shows the engineering stress-strain curves of virgin PTFE and crosslinked PTFE during uniaxial tensile deformation. Mechanical properties of the samples, for example, yield stress, tensile strength, and strain at break, varying with increasing irradiation dose are listed in Table I.

The yield stress and tensile strength of irradiated PTFE increased gradually with increasing irradiation dose, which were obviously higher than those of virgin PTFE. The tensile strength was increased by 72% at 3000 kGy EB-irradiation dose. After EB radiation in the molten state, most of the chains in the specimens were crosslinked[1] and the amorphous network structures were formed. The higher the radiation dose, the more effective amorphous network formed. Therefore, compared to virgin PTFE, the crosslinked PTFE had higher yield strength and tensile strength. The mechanical properties of PTFE were greatly improved by crosslinking using EB irradiation in the molten state. On the contrary, strain at break decreased with increasing irradiation dose. It can be attributed to the ever-increasing 3D gel-like amorphous network structure with irradiation dose, which prevents the structural reorganization during stretching and leads to a decrease in internal chain mobility and elongation.

Morphological Changes for Different Crosslinked PTFE During Deformation

Figure 2 shows the selected SAXS patterns during tensile deformation for virgin PTFE, along with the engineering stress-strain curve. From 0% strain to 12% strain, isotropic scattering patterns were observed. Above extension to 32% strain, an

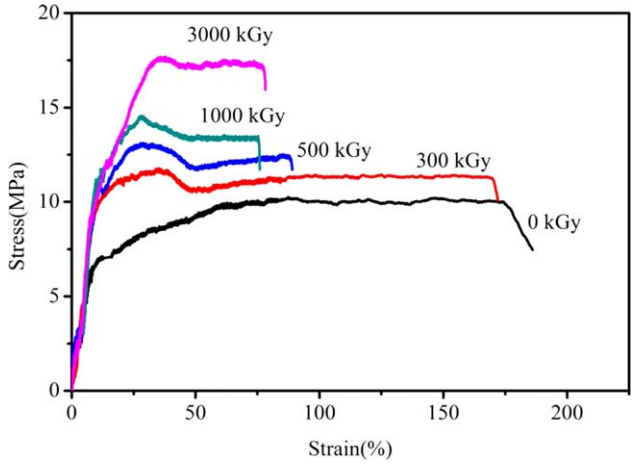

Figure 1. Engineering stress-strain curves of virgin PTFE and crosslinked PTFE. [Color figure can be viewed in the online issue, which is available at wileyonlinelibrary.com.]

Table I. Mechanical Properties of Virgin PTFE and Crosslinked PTFE

Sample code	EB radiation dose (kGy)	Yield stress (MPa)	Tensile stress (MPa)	Strain at break (%)
Virgin PTFE	0	-	9.98	180
XPTFE-300	300	11.78	11.23	169
XPTFE-500	500	13.12	12.40	88
XPTFE-1000	1000	14.45	13.38	76
XPTFE-3000	3000	17.68	17.20	77

anisotropic SAXS pattern appeared and the orientation became obvious with stretching along the meridional direction. It indicated that some amorphous chains were oriented along the pulling axis easily during the stage.[15] Above 140% strain, the SAXS patterns consistently showed a diamond shape. The appearing of these scattering patterns can be attributed to the rod-like structures and voids oriented along the stretching direction.[16,17]

In situ SAXS investigation of PTFE with different crosslinking density was carried out during the stretching processes. Typical SAXS patterns obtained during deformation of XPTFE-3000 (Figure 3) were noticeably different from those of the virgin PTFE. From 0% to 11% strain, an isotropic SAXS pattern was observed and the scattering intensity was almost homogenously distributed. The SAXS pattern showed a broad isotropic ring, which could be interpreted as scattering from randomly oriented stacks of lamellar structure. During stretching, the SAXS pattern changed dramatically with strain. At 22% strain, the scattering ring took on preferred orientation in equatorial direction. After yield point (>35% strain), the SAXS pattern developed into anisotropic elliptical scattering pattern, which may be related to an orientation of distorted lamellar domains. It indicated that the long period of the adjacent lamellae in the stretching direction was larger than that in the meridional direction. (This can also be proved by the long period in Figure 6.) After extension to above 60% strain, four-leaf clover SAXS pattern developed and finally became a four-point pattern at 76% strain; the changed SAXS patterns suggested microdomain distortion.

The integrated SAXS for virgin PTFE and XPTFE-3000 with strain were shown in Figure 4. From the SAXS curves of virgin PTFE [Figure 4(a1,b1)], it can be seen that there was no

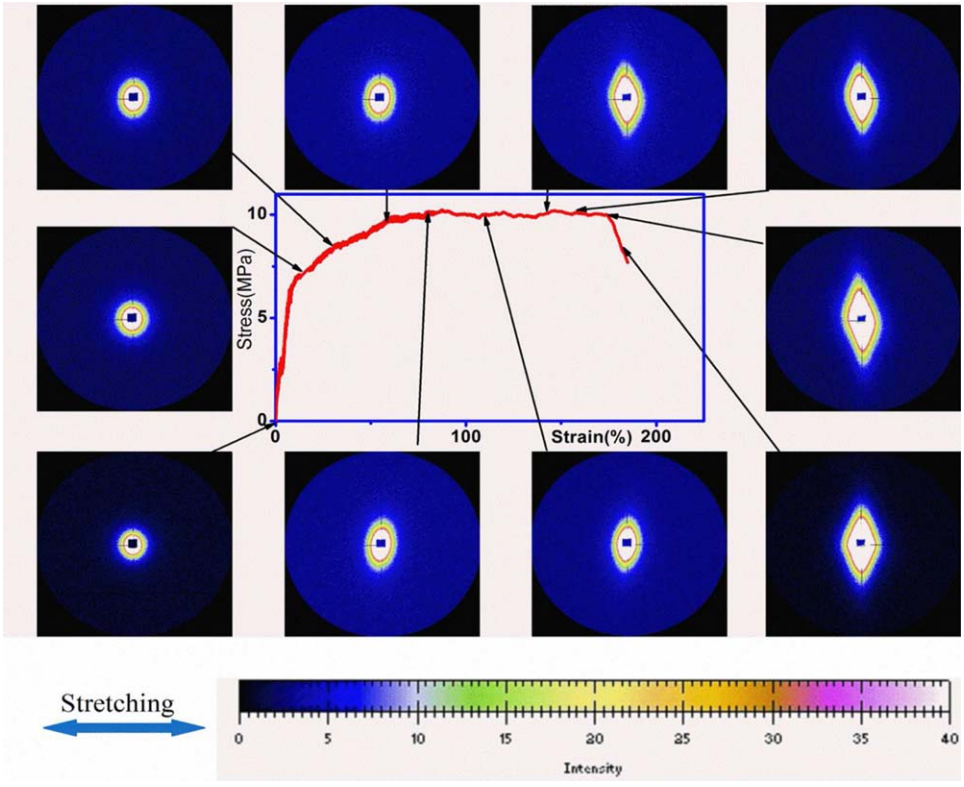

Figure 2. Selected SAXS patterns of virgin PTFE along with the stress-strain curve during tensile stretching at room temperature. The arrows indicated the position where each pattern was taken. [Color figure can be viewed in the online issue, which is available at wileyonlinelibrary.com.]

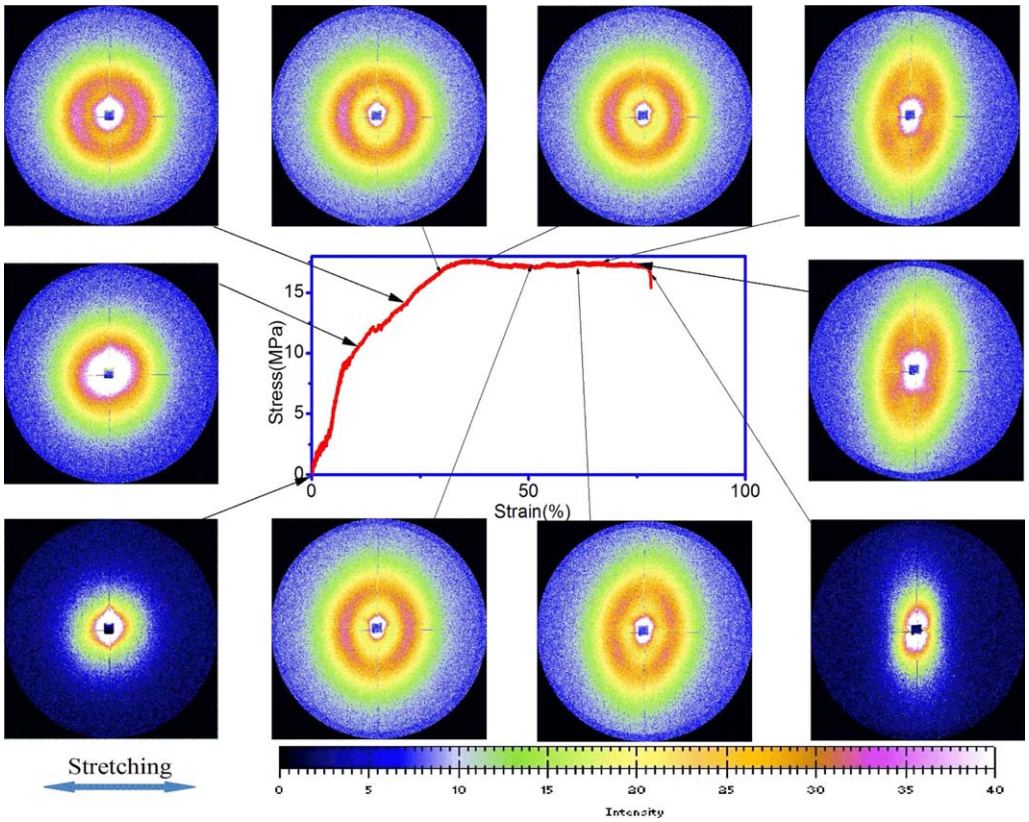

Figure 3. Selected SAXS patterns of crosslinked PTFE with 3000 kGy radiation dose during stretching along with the stress-strain curve. The arrows indicated the average position where each pattern was taken. [Color figure can be viewed in the online issue, which is available at wileyonlinelibrary.com.]

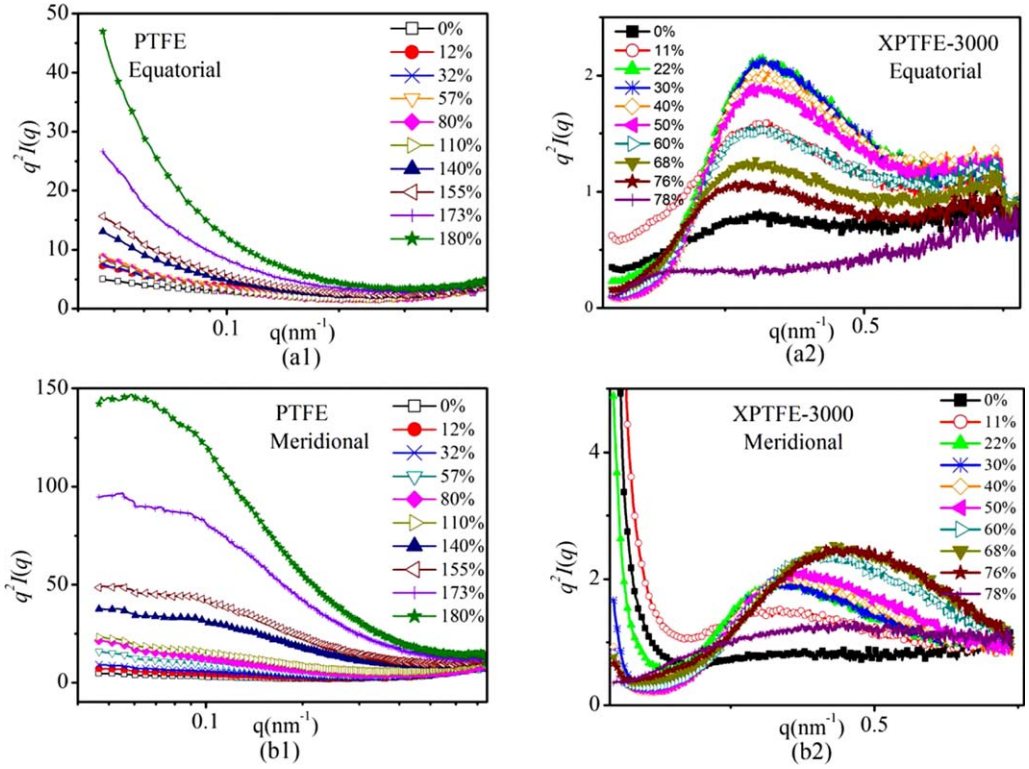

Figure 4. Selected integrated SAXS profiles of PTFE and XPTFE-3000 at different strains. (a1, a2) In the equatorial direction, (b1, b2) in the meridional direction. [Color figure can be viewed in the online issue, which is available at wileyonlinelibrary.com.]

obvious peak existing for virgin PTFE before deformation. It indicated that in virgin PTFE only crystalline lamellae uniformly dispersed in the amorphous matrix and inter-lamellae distances had a very broad distribution. While for the XPTFE-3000 before deformation [Figure 4(a2)], a scattering shoulder appeared at $q = 0.28$ nm^{-1} ($q = 4\pi\sin\theta/\lambda$ with λ being the wavelength and 2θ being the scattering angle) in the equatorial direction, indicating that there were some lamellar domains. During deformation, it can be clearly seen that a sharp peak appeared for XPTFE-3000 in both the equatorial and meridional direction. However, there was only a broad shoulder appearing in the meridional direction above 140% strain for PTFE. It indicated that the lamellar stack periodically in both the equatorial and meridional direction in XPTFE-3000, and crystalline lamellae formed lamellar phase and oriented along the stretching direction above 140% in virgin PTFE.

A detailed structure evolution during deformation of PTFE and XPTFE-3000 was analyzed by *in situ* SAXS. For PTFE, Figure 4 (a1) shows the intensity in equatorial direction had no obvious change below 110% strain and that increased gradually above 140%. Whereas in the meridional direction [Figure 4(b1)], the intensity increased dramatically at the range of 0.05 nm^{-1} $< q <$ 0.1 nm^{-1}. It indicated that the amorphous chains gradually turned to the tensile direction at below 110% strain. Figure 5 shows the ratio of the meridional and equatorial integrated intensity (I_{MR}/I_{EQ},$I_{MR} = \int_0^\infty I(q)\mathrm{d}q$) was >1 and increases gradually with strain. It indicated that during deformation, amorphous chains and some microstructures containing of long fibrils were reoriented along the stretching direction.[18] Probably, there were also small amount of voids after stretching. At high strain, the lamellae slipped in the micronecks and the large lamellar crystal blocks were broken off and incorporated into the newly formed microfibrils, and this has been proved by many researchers.[14,19–23] Brown et al.[8] investigated the morphological change in fracture mechanisms of PTFE, some fibrils (about 10 nm in diameter) and microvoids coalescence were observed. From diamond shape of 2D SAXS pattern, it can be speculated that the microfibrils had a preferred orientation along the stretching direction.

For XPTFE-3000, from the integrated intensity curves of equatorial direction [Figure 4(a2)], in the early stages of deformation before yield point, there was no obvious shift for the lamellar peak position, and only the scattering intensity of the peak became stronger gradually. After yield point (>35% strain), the position of the lamellar peak shifted to lower q in equatorial direction. It indicated that the average spacing of the lamellae parallel to the stretching direction was enlarged due to the elongation of amorphous chains between lamellae crystals. However, the position of the lamellar peak in meridional direction shifted to higher q, as showed in Figure 4(b2). According to Bragg's law, the long period $L = 2\pi/q$. The correlation of long period of XPTFE-3000 with the strain in equatorial and meridional directions is shown in Figure 6. In the meridional direction, the long period decreased slightly and in the equatorial direction it almost did not changed at the early stage before yield point. After yield point (>35% strain), L in the meridional direction decreased monotonously but increased dramatically in the equatorial direction. This result indicated that the tensile deformation enlarged the averages distance between adjacent lamellae in the stretching direction.

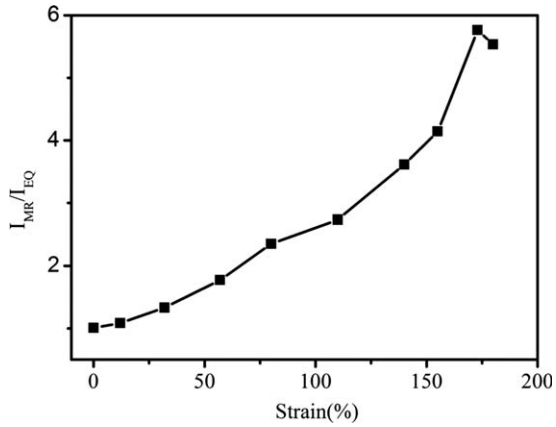

Figure 5. Ratio of the meridional and equatorial intensity with strain.

Effect of Crosslinking Density/Sites on PTFE Structural Change

The SAXS patterns obtained during deformation of virgin/crosslinked PTFE were different from each other. The integrated SAXS at 60% strain for different crosslinked PTFE along the equatorial and meridional direction were shown in Figure 7. For XPTFE-300, a shoulder was observed in both the directions. With increasing crosslinking density, the shoulder became obvious and turned to a peak indicating the lamellae aligned orderly. With increasing crosslinking density, it was not difficult to find that the position of peak shifted to higher q indicating that the long period decreased in both equatorial and meridional directions. It was conceivable that crosslinking density/sites suppressed the chains to crystallize, but the lamellae stacked orderly with increasing crosslinking density.

From SAXS patterns during stretching of different crosslinked PTFE, it was clearly seen that a diamond shape of SAXS pattern appeared at high strain in virgin PTFE, while a four-point SAXS

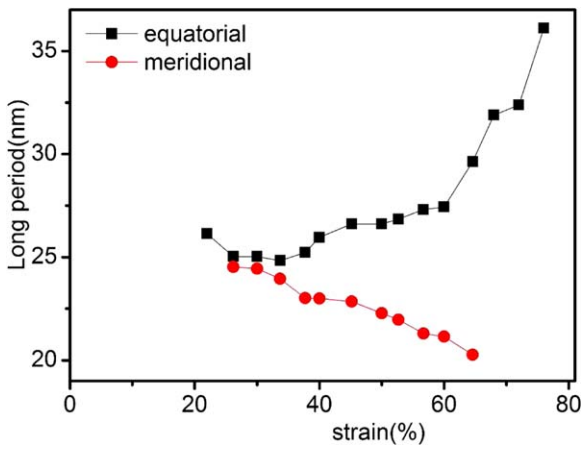

Figure 6. Change of long period L in the equatorial direction (squares) and in the meridional direction (circles) during deformation of XPTFE-3000 (at low strains, the peak is amphibolous, so only high strains display). [Color figure can be viewed in the online issue, which is available at wileyonlinelibrary.com.]

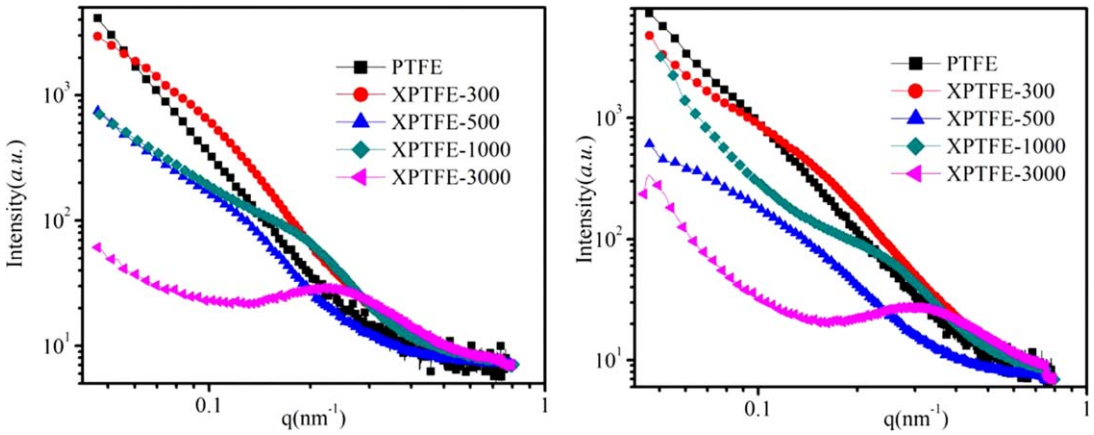

Figure 7. The integrated SAXS profiles of PTFE, XPTFE-300, XPTFE-500, XPTFE-1000, and XPTFE-300 at 60% strain. [Color figure can be viewed in the online issue, which is available at wileyonlinelibrary.com.]

pattern was observed in XPTFE-3000. Three other crosslinked PTFE samples with radiation dose of 300 kGy (XPTFE-300), 500 kGy (XPTFE-500), and 1000 kGy (XPTFE-1000) were studied. Here, the curves of integrated intensity distribution as a function of with the azimuthal angle for different crosslinked PTFE after yield point strain are shown in Figure 8. For virgin PTFE, the SAXS pattern at 140% strain was used to analyze due to its large elongation-to-break ratio, while for crosslinked PTFE, those of 76% strain was taken for example. For I-φ curves, it was obvious that the peak intensity decreased, and the width of peak increased with crosslinking density. Finally one peak split into two weak peaks in XPTFE-3000 from 180° to 360°. To be specific, the high crosslinking density like XPTFE-3000 accelerated the tilting of lamellar stacks in microdomain, and the wider peak indicated that the lamellar structure evolution had a tendency as XPTFE-3000.

In our experiment, the four-point SAXS pattern was only observed in crosslinked PTFE with high radiation dose for first time, but the four-point SAXS pattern had been detected in other materials. Up to now, there were different explanations about the four-point SAXS pattern. Benjamin S. Hsiao and his coworkers proposed two scenarios to explain it.[24] One was that amorphous chains exceed the crystal binding force. This can disintegrate the lamellae structures to smaller lamellar blocks with a checkerboard arrangement. The other was lamellar stacks which were aligned parallel to the stretching direction tend to reorient and tilt. Keith H. D. and Nozue proposed that parent and daughter lamellae formed a cross-hatched structure.[25–27] From the SAXS patterns of crosslinked PTFE, upon stretching, the crystal boundaries and amorphous parts between two neighboring lamellae regularly reoriented and tilted along the stretching direction, That is, an alternately tilted lamella arrangement called herringbone was formed which resulted in the four-point SAXS pattern. Further analysis of the four-point pattern in XPTFE-3000 was carried on to reveal estimates for the tilt angle. An intensity distribution along the elliptical peak as a function of the azimuthal angle φ was plotted (Figure 9). The azimuthal scans for the samples obtained show four-spot pattern where the peaks appeared at about 60°, 110°, 235°, and 285°. From I-φ curves, the four-point SAXS pattern appeared about 60%

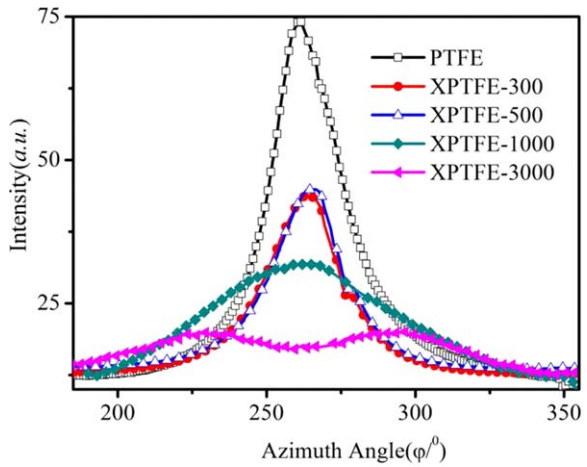

Figure 8. Integrated intensity distribution as a function of the azimuthal angle φ along the elliptical peak for different crosslinked PTFE at high strain (for PTFE 140% strain, for crosslinked PTFE 76% strain). [Color figure can be viewed in the online issue, which is available at wileyonlinelibrary.com.]

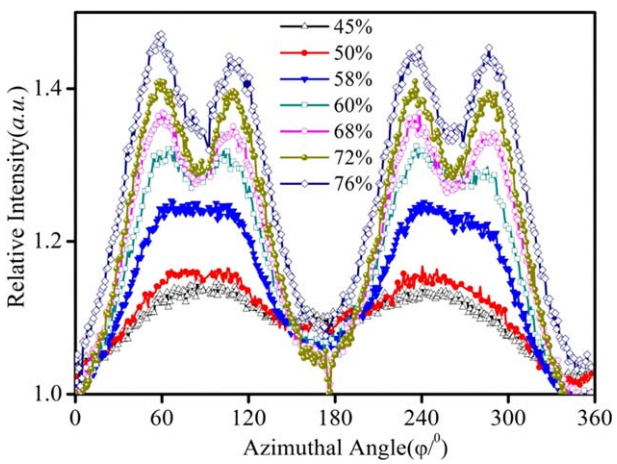

Figure 9. Integrated intensity distribution as a function of the azimuthal angle φ along the elliptical peak for XPTFE-3000. [Color figure can be viewed in the online issue, which is available at wileyonlinelibrary.com.]

strain. During deformation, the first peak shifted to lower angle, μ, was the angle between the lamellar stack and the stretching direction. This meant that μ decreased continuously, indicating the lamellae were gradually aligned along the stretching direction.[28,29] (The value of μ is 65° at 60% strain and reached about 56° at 76% strain). We can calculate the angle (Φ) between two lamellar stacks (Figure 10, XPTFE-3000) from the second and third peaks, and this angle decreased from 60% to 76% strain (Figure 9). The decreasing Φ indicated that lamellar stack reoriented along the stretching direction.

After EB radiation, the yield strength had been improved, referred to our mechanical experiments (Figure 1). Akihiro Oshima proposed that the network formation is helpful to improve the mechanical properties and suppress crystallization.[1,5,6,30] Comparison of SAXS results of different crosslinked PTFE indicates that the different crosslinking network affected the structural evolution during stretching. The deformation process of virgin and crosslinked PTFE can be described using a model illustrated in Figure 10. For virgin PTFE, the crosslinking density was zero. So the mobility of chains is easier than crosslinked PTFE. During deformation, the free long chains transformed into fibrils, microvoids were formed and elongated along stretching direction (Figure 5), and lamellae was destroyed only at high strain. For XPTFE with lower crosslinking density (XPTFE-300 and −500), some crosslinking sites would be destroyed during stretching. So, the lamellar structure stacked orderly and the part of long free chains without crosslinking sites easily transformed into fibrils. However, the crosslinking network among the lamellae is not sufficient to induce lamellar structure slip. For XPTFE with higher crosslinking density such as the XPTFE-3000, the lamellar tilt and reoriented. Since the crosslinking density of XPTFE-3000 was nearly tenfold than those of XPTFE-300, −500, the initial crosslinking sites per chain are higher in XPTFE-3000 than those in XPTFE-300 or 500. The content of network in XPTFE-3000 is tenfold than that of XPTFE-300. Unlike entanglement density, the chains between adjacent crosslinking sites cannot disentangle by itself then crystallize,[31] so during deformation, crosslinking sites broke off; it was inevitable that the lamellar stacks were implicated and tilt by external force because of the high concentration crosslinking network. From the change of width of peak in Figure 8, it was conceivable to speculate the lamellae had a tendency to tilt.

CONCLUSIONS

In this study, *in situ* SAXS experiments coupled with uniaxial stretching were performed to investigate the structural evolution and deformation behavior of virgin and crosslinked PTFE. The results are summarized as follows:

Both the yield and tensile strength of the crosslinked PTFE increased with crosslinking density, but the elongation-to-break ratio decreased due to the formed crosslinking network. For crosslinked PTFE, the long period decreased with the increased crosslinking density. During stretching, for virgin PTFE,

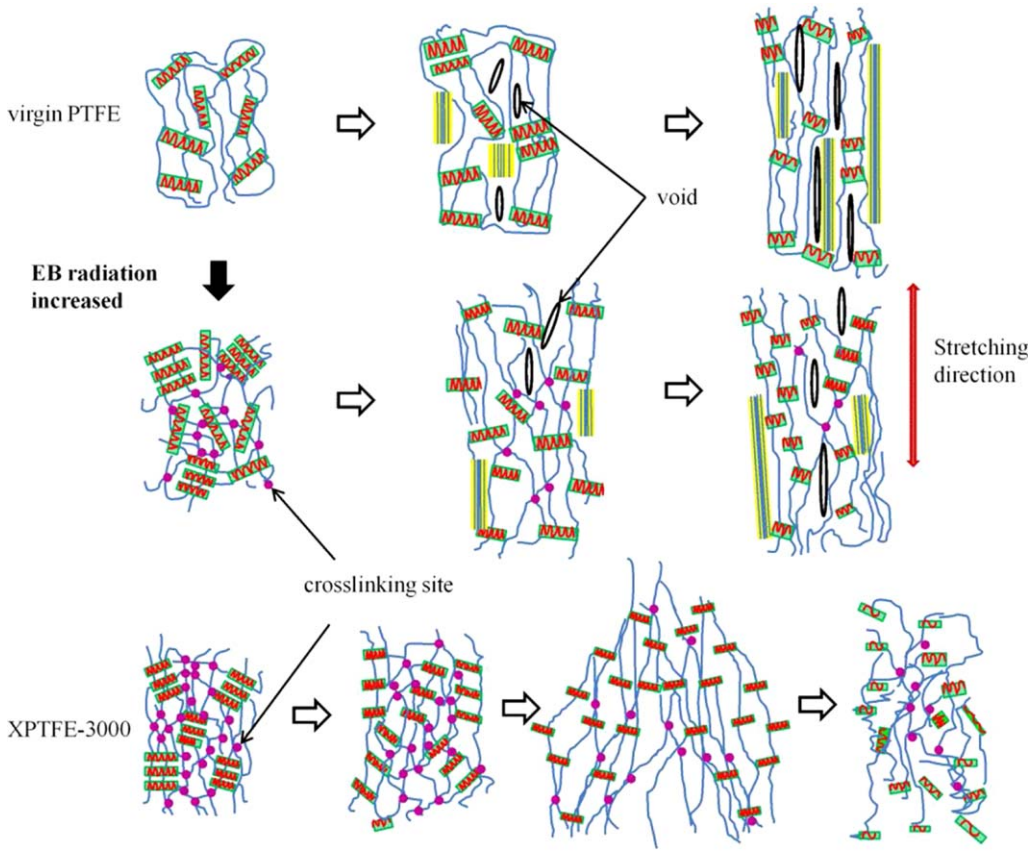

Figure 10. Illustrations of deformation for different radiation dose during uniaxial tensile stretching. [Color figure can be viewed in the online issue, which is available at wileyonlinelibrary.com.]

amorphous chains gradually turned to tensile direction, and the lamellae did not stack periodically initially, but after extension to 140%, crystalline lamellae formed lamellar phase and oriented along the stretching direction. For XPTFE-3000, the lamellar structure slipped, tilted and reoriented during stretching. The four-point SAXS patterns indicate that an alternately tilted lamella arrangement called herringbone structure was formed. While for crosslinked PTFE with low crosslinking density, the four-point SAXS pattern was absent. It was not difficult to analyze that the lamellar structure stacked orderly from their SAXS patterns. Only high concentration crosslinking network on the deformation-induced lamellae slipped and tilted. For virgin PTFE, the fibril and voids formed during deformation. The results verified the effect of crosslinking density can lead to different structure change upon deformation.

ACKNOWLEDGMENTS

The authors acknowledge the financial supports from National Natural Science Foundation of China (Grant Nos. 50903089, 10979073, 11005143, and 10979006) and National Basic Research Program of China (Grant Nos. 2010CB934501,2011CB −606104, and 2011CB605604) and thank Dr. Bian fenggang for discussion.

REFERENCES

1. Oshima, A.; Ikeda, S.; Seguchi, T.; Tabata Y. *Radiat. Phys. Chem.* **1997**, *49*, 279.
2. Forsythe, J. S.; Hill, D. J. T. *Prog. Polym. Sci.* **2000**, *25*, 101.
3. Fayolle, B.; Audouin, L.; Verdu, J. *Polymer* **2003**, *44*, 2773.
4. Sun, J.; Zhang, Y.; Zhong, X.; Zhu, X. *Radiat. Phys. Chem.* **1994**, *44*, 665.
5. Oshima, A.; Tanata, Y.; Kudoh, H.; Seguchi, T. *Radiat. Phys. Chem.* **1995**, *45*, 269.
6. Oshima, A.; Seguchi, T.; Tabata,Y. *Polym. Int.* **1999**, *48*, 996.
7. Oshima, A.; Ikeda, S.; Katoch, E.; Tabata Y. *Radiat. Phys. Chem.* **2001**, *62*, 39.
8. Brown, E. N.; Dattelbaum, D. M. *Polymer* **2005**, *46*, 3056.
9. Brown, E. N.; Dattelbaum, D. M.; Brown, D. W.; Rae, P. *J. Polymer* **2007**, *48*, 2531.
10. Bunn, C. W.; Howells, E. R. *Nature* **1954**, *4429*, 549.
11. Sperati, C. A.; Strarkweather, H. W. Fluorine-Containing Polymers. II. Polytetrafluoroethylene; Springer: Berlin, **1961**, pp 465.
12. Lappan, U.; Geiβler, U.; Lunkwitz, K. *Radiat. Phys. Chem.* **2000**, *59*, 317.
13. Atsuhiro, F.; Yuichiro, H. *Macromolecules* **2008**, *41*, 7606.
14. Choi, K. J.; Spruiell, J. E. *J. Polym. Sci.* **2010**, *48*, 2248.
15. Rae, P. J.; Dattelbaum, D. M. *Polymer* **2004**, *45*, 7615.
16. Gregor, S. D.;*J. Appl. Ploym. Sci.* **2006**, *100*, 1067.
17. Zuo, F.; Keum, J. K.; Chen, X.; Hsiao, B. S.; Chen, H.; Lai, S.;Wevers, R.; Li, J. *Polymer* **2007**, *48*, 6867.
18. Li, X.; Schneider, K.; Krezschmar, B.; Stamm, M. *Macromolecules* **2008**, *41*, 4371.
19. Yang, J.; Williams, R.; Peterson, K.; Geil, P. H.; Long, T.-C.; Xu, P. *Polymer* **2005**, *46*, 8723.
20. Wu, J.; Schultz, J. M.; Yeh, F.; Hsiao, B. S.; Chu, B. *Macromolecules* **2000**, *33*, 1765.
21. Kitamura, T.; Okabe, S.; Tanigaki, M.; Kurumada, K.; Ohshima, M.; Zanazawa, S. *Polym. Eng. Sci* **2000**, *40*, 809.
22. Aglan, H.; Gan, Y.; El-Hadeki, M.; Faughnan, P.; Bryan, C. *J. Mater. Sci.* **1999**, *34*, 83.
23. Joyce, J. *J. Polym. Eng. Sci.* **2003**, *43*, 1702.
24. Liu, L.; Hsiao, B. S.; Fu, B. X.; Ran, S.; Toki, S.; Chu, B.; Tsou, A. H.; Agarwal, P. K. *Macromolecules* **2003**, *36*, 1920.
25. Padden, F. J.; Keith, H. D. *J. Appl. Phys.* **1966**, *37*, 4013.
26. Keith, H. D.; Padden, F. J. *J. Appl. Phys.* **1973**, *44*, 1217.
27. Nozue,Y.; Shinohara, Y.; Ogawa, Y.; Sakurai, T.; Hori, H.; Kasahara, T.; Yamaguchi, N.; Yagi, N.; Amemiya, Y. *Macromolecules* **2007**, *40*, 2036.
28. Rungswang, W.; Kotaki, M.; Shimojima, T.; Kimura, G.; Sakurai, S.; Chirachanchai, S. *Polymer* **2011**, *52*, 844.
29. Chen, X.; Burger, C.; Fang, D.; Sics, I.; Xue, W.; Wei, H.; Somani, R. H.; Kyunghwa, Y.; Hsiao, B. S.; Chu, B. *Macromolecules* **2006**, *39*, 5427.
30. Hougham, G.; Patrick, E. C.; Johns, K.; Theodore, D. *Fluoropolymers 2: Properties Topics in Applied Chemistry*; Kluwer Academic: New York, NY, **1999**.
31. Cai, J.; Hsiao, B. S.; Gross, R. A. *Macromolecules* **2011**, *44*, 3874.